RSC Advances

PAPER

View Article Online
View Journal | View Issue

Open Access Article. Published on 15 November 2022. Downloaded on 11/23/2025 7:24:58 PM.
This article is licensed under a Creative Commons Attribution-NonCommercial 3.0 Unported Licence.

Check for updates

Cite this: *RSC Adv.*, 2022, **12**, 32784

Selective sensing of adenosine monophosphate (AMP) by a calix[6]triazolium-based colorimetric sensing ensemble†

Jihee Cho and Sanghee Kim *

Received 22nd September 2022
Accepted 10th November 2022

DOI: 10.1039/d2ra05987h

rsc.li/rsc-advances

Since adenosine monophosphate (AMP) is closely related to many diseases, the measurement of AMP is important for the diagnosis and treatment of related diseases. Among the AMP sensors reported thus far, sensors that selectively recognize AMP, not ADP or ATP, are rare, and complex experimental procedures and additional instruments are required for AMP recognition. We developed a colorimetric chemosensor using calix[6]triazolium (**CT6**) and intended to use it for the simple and rapid detection of AMP. Colorimetric AMP detection was established through an indicator displacement assay (IDA) in which **CT6** and Brooker's merocyanine (**BM**) were used as receptors and indicators, respectively. The change in the absorption spectrum and color of **BM** showed that the binding affinity of **CT6** to AMP conferred high selectivity to the developed colorimetric chemosensor. The developed IDA-based chemosensor was extended to fabricate a paper-based colorimetric device for visual measurement, and the paper-based device exhibited a selective response to AMP through a definite color change from yellow to magenta. This paper-based colorimetric device shows growth potential for onsite visual measurement of AMP.

Introduction

The development of artificial receptors that can selectively recognize phosphate anions has attracted great interest in supramolecular chemistry because they play critical roles in a wide range of biological processes.[1] Among various biological phosphates, adenosine mono-, di- and triphosphate (AMP, ADP and ATP) are the essential biomolecules, and each has unique functions.[2] AMP, the most fundamental nucleotide, is converted to ADP and ATP by binding with inorganic phosphates during intracellular metabolism. AMP is involved in the regulation of various enzymatic reactions and is a major cellular metabolite that regulates signal transduction and energy homeostasis.[3] The level of AMP in cells is closely related to various diseases. Although many chemosensors for AMP have been reported,[4] chemosensors that selectively recognize AMP over ADP and ATP are rare.[5] In addition, complex experimental procedures and extra equipment are required for AMP recognition.

The indicator displacement assay (IDA) has been widely applied in supramolecular systems to detect various anions.[6] The IDA-based colorimetric sensing system[7] enables the detection of target molecules with the naked eye. Thus, it offers several advantages, such as fast response and simple operation, and does not require expensive analysis equipment. To the best of our knowledge, IDA-based colorimetric systems for the selective detection of AMP over ADP and ATP through distinct color changes have not yet been developed.

Macrocyclic host molecules (MHMs) are ideal receptors for IDA because of their ability to form inclusion complexes with guests.[8] MHMs have preorganized cavities and unique geometries that enhance recognition and selectivity for guest molecules. Recently, various types of MHMs composed of repeating aromatic heterocycles such as imidazolium, pyridinium and triazolium have been reported, and they exhibit distinctive features and recognition ability.[9,10a] Several research groups, including our group, have developed macrocyclic receptors containing 1,2,3-triazolium for anion recognition.[10] The binding properties of triazolium are somewhat different from those of the corresponding 1,2,3-triazole. The anionic binding affinity of triazolium is strongly increased compared to that of triazole because of the cationic character of the former. In addition, the possible anion–π interaction of 1,2,3-triazolium is another important force in the recognition of anionic molecules.[11] Recently, our group synthesized calix[*n*]triazolium composed of multiple triazolium groups.[10a] With this macrocycle, we developed an IDA-based fluorescence-sensing system for the selective detection of AMP. Based on our previous study, we decided to develop a colorimetric chemosensor for AMP.

College of Pharmacy, Seoul National University, 1 Gwanak-ro, Gwanak-gu, Seoul 08826, Korea. E-mail: pennkim@snu.ac.kr

† Electronic supplementary information (ESI) available: ^{1}H NMR studies, complexation studies between **CT6** and **BM**, indicator displacement of the **CT6**/**BM** complex with AMP, detection limit measurements, ^{1}H NMR titration and 2D NOESY NMR studies, competition study and paper-based colorimetric assay. See DOI: https://doi.org/10.1039/d2ra05987h.

© 2022 The Author(s). Published by the Royal Society of Chemistry

Open Access Article. Published on 15 November 2022. Downloaded on 11/23/2025 7:24:58 PM.
This article is licensed under a Creative Commons Attribution-NonCommercial 3.0 Unported Licence.

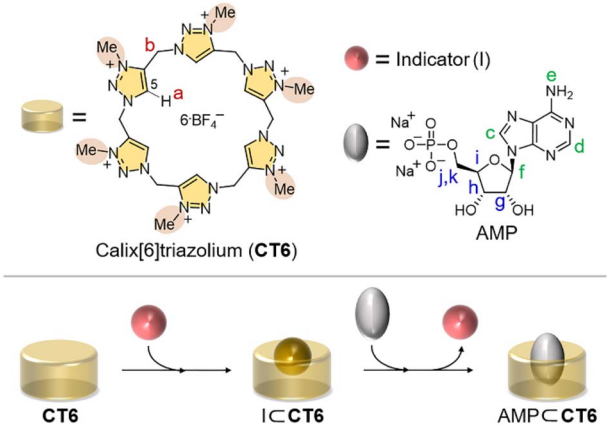

Fig. 1 Schematic illustration of the CT6-based colorimetric indicator displacement assay for AMP. The introduction of AMP is signaled by revived color due to the displacement of the indicator from CT6.

Herein, we report our new macrocyclic detection system for AMP through a color change. Among our calix[*n*]triazoliums (*n* = 4–6), we selected calix[6]triazolium (**CT6**, Fig. 1)[10a] because it displays the best sensitivity to AMP. Brooker's merocyanine (**BM**) was chosen as a colorimetric indicator, and it is known to form a complex with heterocalixarene.[12] Our first working hypothesis is that the color of **BM** changes when a complex is formed with **CT6**. The next hypothesis is that if the interaction of AMP with **CT6** is strong enough to displace **BM** in the **CT6**/**BM** ensemble, it will restore the color of the original **BM** solution.

Results and discussion

We first examined whether the formation of the **CT6**/**BM** complex resulted in a color change. The complexation studies and colorimetric properties of the **CT6**/**BM** complex were studied using UV-Vis spectroscopy. As shown in Fig. 2A, **BM** has absorbance peaks at 256, 392 and 530 nm in DMSO : H_2O (5 : 1) solution. As the concentration of **CT6** increased, the absorbance of **BM** at 256 and 530 nm gradually decreased, while the absorbance at 392 nm gradually increased. The color of the solution changed from magenta to yellow (Fig. 2B). Isotropic points were observed at 322 and 438 nm, indicating that **BM** was complexed with **CT6**. When a hydrogen bond donor (HBD) solvent is added to the **BM** solution, the hypsochromic shift of the absorbance peak of **BM** appears due to the hydrogen bond interaction between the OH of the HBD solvent and the phenolate of **BM**.[13] Therefore, the hypsochromic shift of the absorbance peak of **BM** by the addition of **CT6** suggests that the **CT6**/**BM** complex is formed by hydrogen bonding interactions between **CT6** and the phenolate donor of **BM**. The binding stoichiometric ratio of the **CT6**/**BM** complex was determined to be 1 : 1 by the UV-Vis Job plot method (Fig. S2†). The stoichiometry determined through BindFit calculation was also 1 : 1, and the binding constant of the 1 : 1 binding model was calculated to be 40 402.24 ± 5250 M^{-1} (Fig. S3–S5 and Table S1†).

The complexation of **CT6** with **BM** was also further evaluated by ^{1}H NMR studies (Fig. 3 and S1†). When **CT6** was gradually added to **BM**, all four sets of aromatic protons ($H_{a'}$, $H_{b'}$, $H_{d'}$ and $H_{e'}$) and two sets of alkene protons ($H_{c'}$ and $H_{c''}$) in **BM** shifted

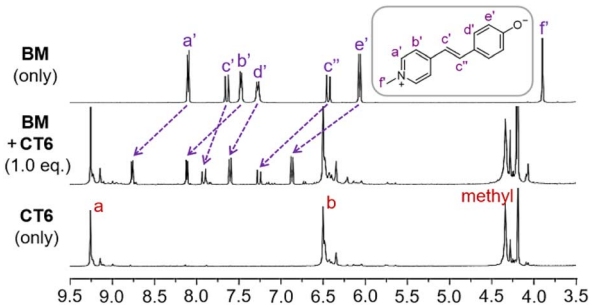

Fig. 3 ^{1}H NMR spectra of **BM** (1.5 mM) in DMSO-d_6 and with **CT6** (1.0 equiv.). The positions of the labeled protons in **CT6** are marked in Fig. 1.

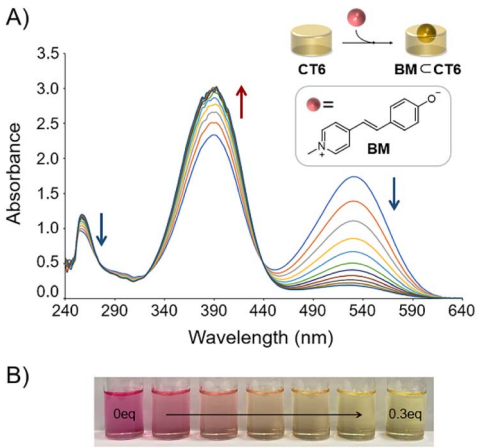

Fig. 2 (A) UV-Vis titration of **BM** (100 μM) upon addition of **CT6** (0–0.3 equiv.) in DMSO : H_2O (5 : 1) solution. (B) Progressive color change of **BM** (100 μM) with an increasing amount of **CT6** (0–0.3 equiv.) in DMSO : H_2O (5 : 1) solution.

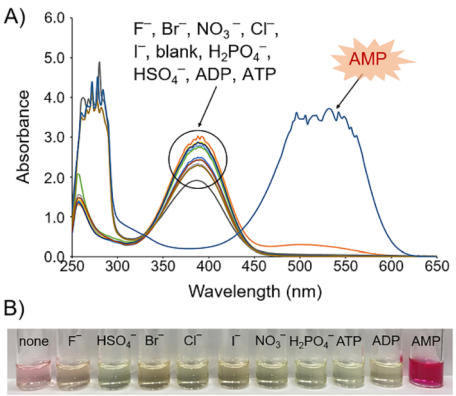

Fig. 4 (A) UV-Vis spectra of the **CT6**/**BM** complex (100 μM) in the presence of 100 equiv. of various anions in DMSO : H_2O (5 : 1) solution. (B) Changes in the color of the **CT6**/**BM** complex (1 mM) in the presence of 100 equiv. of various anions in DMSO : H_2O (5 : 1) solution.

Open Access Article. Published on 15 November 2022. Downloaded on 11/23/2025 7:24:58 PM.
This article is licensed under a Creative Commons Attribution-NonCommercial 3.0 Unported Licence.

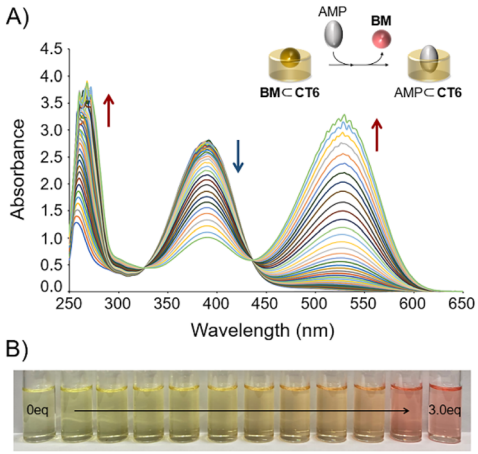

Fig. 5 (A) UV-Vis spectra of the **CT6/BM** complex (100 μM) upon addition of AMP (0–5.0 equiv.) in DMSO : H_2O (5 : 1) solution. (B) Progressive color change of the **CT6/BM** complex (100 μM) with an increasing amount of AMP (0–3.0 equiv.) in DMSO : H_2O (5 : 1) solution.

downfield, indicating an intimate interaction between **CT6** and **BM**.

We next examined whether AMP displaces **BM** in the **CT6/BM** ensemble. When AMP was added to the **CT6/BM** complex, a significant change was observed in the absorption spectrum (Fig. 4A), and the color of the solution changed from yellow to magenta (Fig. 4B). In contrast, the addition of other anions of the same concentration (such as sodium salts, F^-, Cl^-, Br^-, I^-, $H_2PO_4^-$, NO_3^-, HSO_4^-, ADP or ATP) did not significantly affect the absorption spectrum of the **CT6/BM** complex and did not induce the color change (Fig. 4A and B). In particular, other adenine nucleotides, ADP and ATP, did not cause any notable changes in the **CT6/BM** complex.

A titration experiment was performed to determine the binding properties of the **CT6/BM** complex to AMP. As shown in Fig. 5A, when AMP was gradually added to the **CT6/BM** complexes, the absorbance peak at 392 nm gradually decreased, while the absorbance peaks at 256 and 530 nm gradually increased. It also showed a gradual color change from yellow to magenta (Fig. 5B). Isotropic points were observed at 328 and 438 nm. These observations suggested that **BM** bound to **CT6** was released in an AMP-dependent manner. As a result of the BindFit calculation performed using UV-Vis titration of the **CT6/BM** complex with AMP, the stoichiometry was determined to be 1 : 1, and the binding constant of the 1 : 1 binding model was calculated to be 2808.94 ± 54 M^{-1} (Fig. S6–S8 and Table S2†). In addition, the UV-Vis limit of detection (LOD) for AMP of the **CT6/BM** complex was determined to be 30 nM, which is significantly lower than the values reported for other AMP sensors (Fig. S9†).[5e,14,15]

Our previous experiments of ^{1}H NMR titration[10a] revealed that triazolium C5 proton (H_a) of **CT6** and protons (H_{g-k}) adjacent to the phosphate group of AMP shifted downfield, while adenine protons (H_{c-e}) and proton (H_f) adjacent to adenine tended to move upfield (Fig. S10†). This result implied that the binding between **CT6** and AMP occurs *via* hydrogen bonding of triazolium C5–H with phosphate group as well as cation–π interaction between the triazolium ring and the adenine base. In addition to this, we performed 2D NOESY analysis (Fig. S11†). NOESY spectra of AMP were recorded in the presence of **CT6** (0.5 equiv.). An NOE correlation signal was observed between triazolium C5 proton (H_a) of **CT6** and a proton (H_i) adjacent to the phosphate group of AMP. This result suggests a spatially close interaction between **CT6** and AMP.

To investigate the selective recognition ability of **CT6/BM** complex for AMP, a competition experiment was performed in the presence of interfering anions (sodium salts, F^-, Cl^-, Br^-, I^-, $H_2PO_4^-$, NO_3^-, HSO_4^-, ADP or ATP) (Fig. 6 and S12†). When 10 equiv. of anions were added to the **CT6/BM** complex solution containing AMP (30 equiv.), no significant effect was observed on absorbance and color. When 20 equiv. of anions were added, only HSO_4^- and ATP affected the absorbance. HSO_4^- and ATP showed 94% and 83% decrease in absorbance, respectively. When the concentration of anions was increased to 30 equiv., HSO_4^-, ATP and ADP caused notable changes. ADP exhibited 68% decrease in absorbance and slight color change, whereas HSO_4^- and ATP showed a great decrease (>95%) in absorbance and obvious color change from magenta to yellow. These results indicate that the **CT6/BM** complex is highly selective for AMP in the presence of most interfering anions, although the selectivity of the **CT6/BM** complex is affected by the concentration of a few anions.

To show the practical applicability of our colorimetric IDA system, a paper-based device was fabricated. For this, the test paper disc was immersed in **CT6/BM** complex solution for approximately 5 minutes and then dried under vacuum. A solution containing various anions (sodium salts, F^-, Cl^-, Br^-, I^-, $H_2PO_4^-$, NO_3^-, HSO_4^-, AMP, ADP or ATP) was added to a dried test paper disc to confirm its anion selectivity. As shown

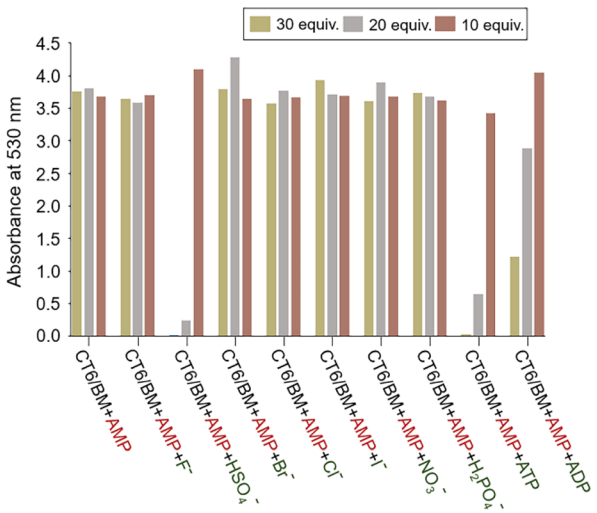

Fig. 6 UV-Vis absorbance response profiles of **CT6/BM** complex (100 μM) at 530 nm in the presence of AMP (30 equiv.) with varying concentrations (10, 20 and 30 equiv.) of interfering anions in DMSO : H_2O (5 : 1) solution.

 © 2022 The Author(s). Published by the Royal Society of Chemistry

Open Access Article. Published on 15 November 2022. Downloaded on 11/23/2025 7:24:58 PM.
This article is licensed under a Creative Commons Attribution-NonCommercial 3.0 Unported Licence.

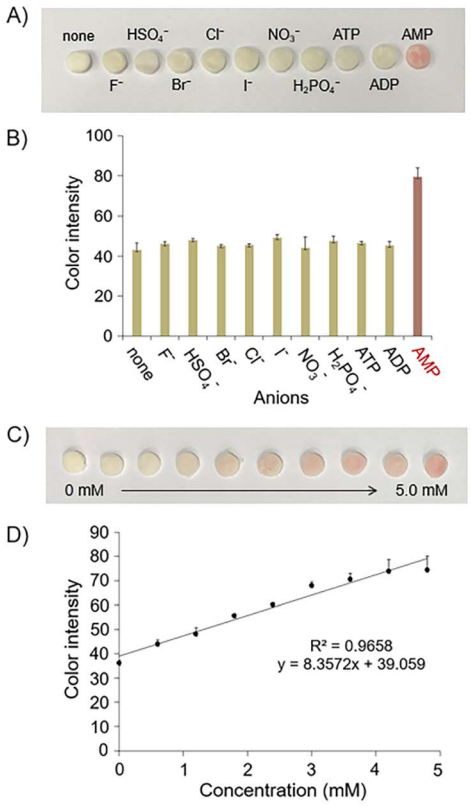

Fig. 7 CT6/BM complex-coated paper discs used for AMP detection. (A) Visible color change and (B) color bar intensity of CT6/BM complex-coated paper discs in the presence of various anions (5 mM). (C) Progressive visible color change and (D) color intensity of CT6/BM complex-coated paper discs in the presence of various concentrations of AMP (0–5.0 mM). The images of paper discs acquired by a smartphone (iPhone 11) were processed using ImageJ software, and the error bars represent the standard deviation of three independent measurements.

in Fig. 7A and B, only AMP showed a clear color change from yellow to magenta, while the other anions tested, including ATP and ADP, did not cause any color changes. To examine the correlation between the color change of the paper disc and the amount of AMP, various concentrations of AMP were added to the paper disc. Paper disc showed a magenta color with increasing color intensity as the AMP concentration increased (Fig. 7C). After images of the paper disc were acquired using a smartphone (iPhone 11), quantitative image processing was performed with ImageJ software (see Section 7 in the ESI†). The color intensity obtained from the image was plotted against the concentration of AMP. As shown in Fig. 7D, the color intensity of the paper disc increased as a function of AMP concentration. The sensitivity of the paper-based AMP sensing device was sufficiently high to allow the detection of even 1.8 mM AMP with the naked eye.

A paper disc was applied to determine the level of AMP in an artificially mixed sample composed of AMP and other anions (F^-, Cl^-, Br^- and I^-) (Table S3 and Fig. S13†). Paper discs measured in a mixed sample containing 2.7 mM AMP and other anions showed a color change from yellow to magenta. The resulting color signal was converted to color intensity by ImageJ. This color intensity was applied to the calibration curve (Fig. 7D) constructed by the pure AMP sample. The AMP concentration thus determined was 2.6 mM, which matches well with the AMP concentration used in the mixed sample. This result suggests that the coexistence of other anions did not hamper AMP detection with the paper disc. These results show the reliability of the fabricated paper disc and its applicability to real samples.

Conclusions

In summary, we developed a novel colorimetric IDA-based chemosensor using **CT6** for the selective detection of AMP. **CT6** was complexed with **BM** with 1 : 1 stoichiometry, which was accompanied by a change in the UV-Vis absorption spectrum and a color change from magenta to yellow. The addition of AMP to the **CT6**/**BM** complex regenerated the original color of **BM**, magenta, and the original absorption spectrum, owing to the release of **BM** through AMP recognition of **CT6**. **CT6** was complexed with AMP at 1 : 1 stoichiometry, which was determined by BindFit calculation. The colorimetric response provided by the IDA-based chemosensor was extended to the simple paper-based device. The fabricated paper-based device exhibited a selective color change only in the presence of AMP, providing a convenient and reliable method for AMP measurement. The developed colorimetric chemosensor has great potential as a new tool for field measurement of AMP. To extend the results of this study, our group is currently working on a paper-based sensor coupled with a smartphone for the sensitive and selective measurement of AMP in biological samples.

Author contributions

J. Cho performed all experimental work and wrote the manuscript and ESI.† S. Kim provided supervision and wrote the manuscript. All authors have read and approved the final version of the manuscript.

Conflicts of interest

There are no conflicts of interest to declare.

Acknowledgements

This work was supported by Grant no. 2018R1A5A2024425 (S. K.) of the National Research Foundation (NRF) funded by the Korean government (MSIT). This research was also supported by the Basic Science Research Program through the National Research Foundation of Korea (NRF) funded by the Ministry of Education (no. 2020R1I1A1A01073399, J. C.).

References

1 A. E. Hargrove, S. Nieto, T. Zhang, J. L. Sessler and E. V. Anslyn, Artificial receptors for the recognition of

Open Access Article. Published on 15 November 2022. Downloaded on 11/23/2025 7:24:58 PM.
This article is licensed under a Creative Commons Attribution-NonCommercial 3.0 Unported Licence.

phosphorylated molecules, *Chem. Rev.*, 2011, **111**, 6603–6782.

2 (*a*) B. S. Khakh and G. Burnstock, The double life of ATP, *Sci. Am.*, 2009, **301**, 84–92; (*b*) C. G. Nichols, S.-L. Shyng, A. Nestorowicz, B. Glaser, J. P. Clement, G. Gonzalez, L. Aguilar-Bryan, M. A. Permutt and J. Bryan, Adenosine diphosphate as an intracellular regulator of insulin secretion, *Science*, 1996, **272**, 1785–1787.

3 (*a*) D. Carling, F. V. Mayer, M. J. Sanders and S. J. Gamblin, AMP-activated protein kinase: nature's energy sensor, *Nat. Chem. Biol.*, 2011, **7**, 512–518; (*b*) E. Helmreich and C. F. Cori, The role of adenylic acid in the activation of phosphorylase, *Proc. Natl. Acad. Sci. U. S. A.*, 1964, **51**, 131–138; (*c*) T. E. Mansour, Studies on heart phosphofructokinase: purification, inhibition and activation, *J. Biol. Chem.*, 1963, **238**, 2285–2292.

4 For recent examples, see: (*a*) I. Carreira-Barral, I. Fernández-Pérez, M. Mato-Iglesias, A. De Blas, C. Platas-Iglesias and D. Esteban-Gómez, Recognition of AMP, ADP and ATP through cooperative binding by Cu(II) and Zn(II) complexes containing urea and/or phenylboronic-acid moieties, *Molecules*, 2018, **23**, 479; (*b*) J. González-García, S. Tomić, A. Lopera, L. Guijarro, I. Piantanida and E. García-España, Aryl-bis-(scorpiand)-aza receptors differentiate between nucleotide monophosphates by a combination of aromatic, hydrogen bond and electrostatic interactions, *Org. Biomol. Chem.*, 2015, **13**, 1732–1740; (*c*) S. Nadella, J. Sahoo, P. S. Subramanian, A. Sahu, S. Mishra and M. Albrecht, Sensing of phosphates by using luminescent Eu^{III} and Tb^{III} complexes: application to the microalgal cell *Chlorella vulgaris*, *Chem.–Eur. J.*, 2014, **20**, 6047–6053; (*d*) P. Hu, S. Yang and G. Feng, Discrimination of adenine nucleotides and pyrophosphate in water by a zinc complex of an anthracene-based cyclophane, *Org. Biomol. Chem.*, 2014, **12**, 3701–3706; (*e*) S. Nadella, P. M. Selvakumar, E. Suresh, P. S. Subramanian, M. Albrecht, M. Giese and R. Fröhlich, Lanthanide(III) complexes of bis-semicarbazone and bis-imine-substituted phenanthroline ligands: solid-state structures, photophysical properties, and anion sensing, *Chem.–Eur. J.*, 2012, **18**, 16784–16792.

5 For selected examples, see: (*a*) K. Kanagaraj, C. Xiao, M. Rao, C. Fan, V. Borovkov, G. Cheng, D. Zhou, Z. Zhong, D. Su, X. Yu, J. Yao, T. Hao, W. Wu, J. J. Chruma and C. Yang, A quinoline-appended cyclodextrin derivative as a highly selective receptor and colorimetric probe for nucleotides, *iScience*, 2020, **23**, 100927; (*b*) Y. Zhao, D. Niu, J. Tan, Y. Jiang, H. Zhu, G. Ouyang and M. Liu, Alkaline-earth metal ion turn-on circularly polarized luminescence and encrypted selective recognition of AMP, *Small Methods*, 2020, **4**, 2000493; (*c*) R. L. Narendran and A. Patnaik, Synergistic effect of hydrophobic and hydrogen bonding interaction-driven viologen-pyranine charge-transfer aggregates: adenosine monophosphate recognition, *Soft Matter*, 2021, **17**, 903–914; (*d*) L. Reinke, M. Koch, C. Müller-Renno and S. Kubik, Selective sensing of adenosine monophosphate (AMP) over adenosine diphosphate (ADP), adenosine triphosphate (ATP), and inorganic phosphates with zinc(II)-dipicolylamine-containing gold nanoparticles, *Org. Biomol. Chem.*, 2021, **19**, 3893–3900; (*e*) R. Kaur, S. Saini, N. Kaur, N. Singh and D. O. Jang, Rhodamine-based fluorescent probe for sequential detection of Al^{3+} ions and adenosine monophosphate in water, *Spectrochim. Acta, Part A*, 2020, **225**, 117523–117531.

6 A. C. Sedgwick, J. T. Brewster, T. Wu, X. Feng, S. D. Bull, X. Qian, J. L. Sessler, T. D. James, E. V. Anslyn and X. Sun, Indicator displacement assays (IDAs): the past, present and future, *Chem. Soc. Rev.*, 2021, **50**, 9–38.

7 B. T. Nguyen and E. V. Anslyn, Indicator-displacement assays, *Coord. Chem. Rev.*, 2006, **250**, 3118–3127.

8 (*a*) Z. Zheng, S. Ren, W.-C. Geng, X. Cui, B. Wu and H. Wang, Monitoring methionine decarboxylase by a supramolecular tandem assay, *Chem.–Asian J.*, 2022, **17**, e202200106; (*b*) W. Zhong and R. J. Hooley, Combining excellent selectivity with broad target scope: biosensing with arrayed deep cavitand hosts, *Acc. Chem. Res.*, 2022, **55**, 1035–1046; (*c*) Y.-C. Pan, X.-Y. Hu and D.-S. Guo, Biomedical applications of calixarenes: state of the art and perspectives, *Angew. Chem., Int. Ed.*, 2021, **60**, 2768–2794.

9 (*a*) X. Chi, W. Cen, J. A. Queenan, L. Long, V. M. Lynch, N. M. Khashab and J. L. Sessler, Azobenzene-bridged expanded "texas-sized" box: a dual-responsive receptor for aryl dianion encapsulation, *J. Am. Chem. Soc.*, 2019, **141**, 6468–6472; (*b*) S. Kosiorek, H. Butkiewicz, O. Danylyuk and V. Sashuk, Pillar[6]pyridinium: a hexagonally shaped molecular box that selectively recognizes multicharged anionic species, *Chem. Commun.*, 2018, **54**, 6316–6319.

10 (*a*) J. Cho, J. Shin, M. Kang, P. Verwilst, C. Lim, H. Yoo, J. G. Kim, X. Zhang, C. S. Hong, J. S. Kim and S. Kim, Calix[*n*]triazolium based turn-on fluorescent sensing ensemble for selective adenosine monophosphate (AMP) detection, *Chem. Commun.*, 2021, **57**, 12139–12142; (*b*) J. Cho, P. Verwilst, M. Kang, J.-L. Pan, A. Sharma, C. S. Hong, J. S. Kim and S. Kim, Crown ether-appended calix[2]triazolium[2]arene as a macrocyclic receptor for the recognition of the $H_2PO_4^-$ anion, *Chem. Commun.*, 2020, **56**, 1038–1041; (*c*) M. S. Shad, P. V. Santhini and W. Dehaen, 1,2,3-Triazolium macrocycles in supramolecular chemistry, *Beilstein J. Org. Chem.*, 2019, **15**, 2142–2155.

11 F. Zapata, L. Gonzalez, A. Caballero, I. Alkorta, J. Elguero and P. Molina, Dual role of the 1,2,3-triazolium ring as a hydrogen-bond donor and anion–π receptor in anion-recognition processes, *Chem.–Eur. J.*, 2015, **21**, 9797–9808.

12 M. M. Linn, D. C. Poncio and V. G. Machado, An anionic chromogenic sensor based on the competition between the anion and a merocyanine solvatochromic dye for calix[4]pyrrole as a receptor site, *Tetrahedron Lett.*, 2007, **48**, 4547–4551.

13 T. Bevilaqua, D. C. da Silva and V. G. Machado, Preferential solvation of Brooker's merocyanine in binary solvent mixtures composed of formamides and hydroxylic solvents, *Spectrochim. Acta, Part A*, 2004, **60**, 951–958.

 © 2022 The Author(s). Published by the Royal Society of Chemistry

Open Access Article. Published on 15 November 2022. Downloaded on 11/23/2025 7:24:58 PM.
This article is licensed under a Creative Commons Attribution-NonCommercial 3.0 Unported Licence.

14 (*a*) R. Kumar, H. Jain, P. Gahlyan, A. Joshi and C. N. Ramachandran, A highly sensitive pyridine-dicarbohydrazide based chemosensor for colorimetric recognition of Cu^{2+}, AMP^{2-}, F^{-} and AcO^{-} ions, *New J. Chem.*, 2018, **42**, 8567–8576; (*b*) D. Datta, X. Meshik, S. Mukherjee, K. Sarkar, M. S. Choi, M. Mazouchi, S. Farid, Y. Y. Wang, P. J. Burke, M. Dutta and M. A. Stroscio, Submillimolar detection of adenosine monophosphate using graphene-based electrochemical aptasensor, *IEEE Trans. Nanotechnol.*, 2017, **16**, 196–202; (*c*) H. Gao, M. Xi, X. Qi, M. Lu, T. Zhan and W. Sun, Application of a hydroxyl functionalized ionic liquid modified electrode for the sensitive detection of adenosine-5′-monophosphate, *J. Electroanal. Chem.*, 2012, **664**, 88–93; (*d*) Y. Song, C. Zhao, J. Ren and X. Qu, Rapid and ultra-sensitive detection of AMP using a fluorescent and magnetic nano-silica sandwich complex, *Chem. Commun.*, 2009, 1975–1977; (*e*) L. Shen, Z. Chen, Y. Li, P. Jing, S. Xie, S. He, P. He and Y. Shao, A chronocoulometric aptamer sensor for adenosine monophosphate, *Chem. Commun.*, 2007, 2169–2171; (*f*) S. Mondal, K. Hsiao and S. A. Goueli, Utility of adenosine monophosphate detection system for monitoring the activities of diverse enzyme reactions, *Assay Drug Dev. Technol.*, 2017, **15**, 330–341.

15 To the best of our knowledge, only two AMP sensors have lower LOD values than the **CT6**/**BM** ensemble. See: ref. 5*e* and 14*f*.